GEOPERSIA

Accepted Manuscript

Petroleum geochemical characterization of the Middle Jurassic Sargelu oil shale, Zagros Mountains, Southwest Iran: Implications for petroleum system analysis

Ali Shekarifard, Dag A. Karlsen, Manouchehr Daryabandeh, Mehrab Rashidi

DOI: 10.22059/GEOPE.2024.380080.648765

Receive Date: 29 July 2024
Revise Date: 29 September 2024
Accept Date: 19 October 2024

Petroleum geochemical characterization of the Middle Jurassic Sargelu oil shale, Zagros Mountains, Southwest Iran: Implications for petroleum system analysis

Ali Shekarifard [1, *], Dag A. Karlsen [2], Manouchehr Daryabandeh [3], Mehrab Rashidi [3]

[1] Institute of Petroleum Engineering (IPE), School of Chemical Engineering, College of Engineering, University of Tehran, Tehran, Iran
[2] Department of Geosciences, University of Oslo, Oslo, Norway, P.O. Box 1047 Blindern, N-0316 Norway
[3] Exploration Directorate, National Iranian Oil Company (NIOC), Tehran, Iran

Received: 29 July 2024, Revised: 29 September 2024, Accepted: 19 October 2024

Abstract
Two main oil shale intervals are recognized in the Qalikuh area of the Zagros Mountains in Lorestan Province, SW Iran: a lower oil shale in the Middle Jurassic Sargelu Formation, and an upper oil shale in the Early Cretaceous Garau Formation. In the present study, 50 outcrop samples of the Sargelu oil shale were collected from eight different localities and were subjected to a complete set of organic geochemical analyses. Samples of the Sargelu oil shale analysed exhibit high organic carbon (TOC) contents (mean: 15.5 wt%). The hydrogen index (mean: 548 mg HC/g TOC) and the genetic potential (mean: 86.20 mg HC/g rock) for the samples represent highly oil-prone kerogen. The Sargelu oil shale is enriched in sulfur, and elemental hydrogen has a moderate-to-high content. Organic petrography shows that the samples are dominated by solid bitumen and carbonate minerals, and X-ray fluorescence analysis shows that the main inorganic component of the oil shale is calcite. The palynofacies are characterized nearly entirely by amorphous organic matter. Kerogen in the Sargelu oil shale is Type II-S. In terms of thermal maturity, there is consistency between vitrinite reflectance, elemental analysis, and thermal maturity-related biomarker parameters which confirm that the Sargelu oil shale is located in the early stage of the oil window (Rc=0.8%). This study shows that there is little significant difference in the geochemical and mineralogical properties of the Garau and Sargelu oil shales from Qalikuh, or in their respective pyrolysate products, despite the formations' different stratigraphies and ages. However, compared to Garau-derived oils (extracts), the Sargelu-derived oils (extracts) demonstrate a higher ratio of dibenzothiophene to phenanthrene (DBP/Phen) and a lower ratio of C_{27}/C_{29} sterane. These parameters can in future be used in oil - source rock correlation studies in locations where these formations are deeply buried and highly mature, and where the precise contribution of hydrocarbons from Sargelu and Garau source rocks to a reservoired petroleum is unknown.

Keywords: Petroleum geochemistry, oil shale, Jurassic, Zagros fold-and-thrust belt, Iran.

Introduction

The carbonate-dominated Middle Jurassic Sargelu and Early Cretaceous Garau Formations include high quality organic-rich source rocks (SRs) at oil fields both in SW Iran (e.g. Darquain,

* Corresponding author e-mail: ashekary@ut.ac.ir

Azadegan, Juffair and Yadavaran) and in neighboring countries (cf. Murris 1980; Bordenave and Burwood 1990; Mahbobipour et al. 2016).

The Middle Jurassic SRs were deposited in an anoxic intrashelf basin (Klemme 1994; Ziegler 2001; Abdula 2015; Wilson 2020) from the end of the Lias to the end of the Bathonian. In the Zagros Fold belt of Iran there are mainly five petroleum systems including the Middle Jurassic and Early Cretaceous. In the Middle Jurassic petroleum system (PS), some oil derived from the Sargelu SRs has migrated to reservoir rocks along the margins of the depression, but a significant portion of the oil generated was not expelled and was instead broken down in situ into pyrobitumen and gas. Some oil migrated laterally into the porous platform facies of the Surmeh–Khami Formations, accumulated on regional highs prior to the Zagros folding, and then migrated into Zagros folds (Bordenave and Hegre 2010). It is worth mentioning that cumulative isopachs imply that during the commencement of the Zagros folding, the central Lorestan Depression's Sargelu Formation had already expelled the majority of its oil and entered the gas phase (Bordenave and Hegre 2010).

The Early Cretaceous PS was charged by outstanding SRs deposited during the Neocomian at the base of the Garau Formation. The Early Cretaceous PS is another illustration of SRs that are not or poorly associated with reservoirs, as a major portion of the oil produced was broken in situ into pyrobitumen and gas. Concerning the Middle Jurassic PS, some oil moved laterally into the porous platform facies of the Khami reservoirs, accumulated on regional highs prior to the Zagros folding, and then migrated into Zagros folds (Bordenave and Hegre 2010).

It was an Early Jurassic depression that persisted through the Mesozoic over NE-Iraq and Lorestan (Murris 1980; Ayres et al. 1982). Anoxic conditions developed in the Lorestan Basin during the Middle Jurassic to Middle Cretaceous times. Similar depositional conditions occurred in the Dezful Embayment and in the N Persian Gulf, where the Sargelu Formation was deposited. The large and extensive deep-water Sargelu-Gotina Basin was the depositional locus for high-quality argillaceous carbonate SRs (Murris 1980; Ayres et al. 1982). Similar to the Garau Formation, oxygen-poor conditions in the Sargelu Formation led to the development of a thick black organic-rich interval within the formations, namely, the high stand facies (e.g., Murris 1980; Ziegler 2001; Van Buchem et al. 2010).

Nearly all previous evaluations in the Zagros Basin (Fig. 1) show the organic-rich facies from the Sargelu and Garau formations are deeply buried and highly matured with a relatively good range of total organic carbon, namely, total organic carbon (TOC) < 6.5 wt% (e.g., Ala et al. 1980; Bordenave and Huc 1995; Kamali and Rezaee 2003). Our present and earlier studies (Shekarifard et al. 2019) in the Qalikuh area from Lorestan Province of the High Zagros (thrust belt) of the Zagros Mountains (Fig. 1a) confirm the especial occurrence of organic-rich facies from the Sargelu and Garau formations. In this area, these organic-facies show the highest amount of TOC and the lowest level of thermal maturity which are cropped out at the surface (Rasouli et al. 2015; Shekarifard et al. 2019). In Qalikuh area, these organic-facies intervals are called oil shale (Shekarifard et al. 2019). Oil shale is a type of extremely kerogen-rich SR with low maturity that can be mined and utilized for oil extraction (Tissot and Welte 1984).

In the Jurassic-Cretaceous petroleum systems of SW Iran, where the Cretaceous and younger reservoirs were charged by these Jurassic-Cretaceous SRs, the main challenging problem is the oil-source correlation investigation in locations where these SRs are deeply buried and highly mature, and where the precise contribution of hydrocarbons from the Sargelu and Garau SRs to a reservoired petroleum is unknown. Accordingly, main aim of this study is to solve this problem by focusing on characterizing and comparing the organic matter (i.e., solvent extract and kerogen) from the Sargelu and Garau oil shale in the Qalikuh area, where maturity is known to be low. Therefore, the geochemical characterization of these oil shales is highly important for a better understanding of Iran’s Jurassic-Cretaceous petroleum systems, where these formations have acted as effective SRs. This may further contribute to the understanding of the

oil-SR correlation and to get better approach for oil-fields developments.

Geology and lithostratigraphy

The Lorestan province, comprising the Qalikuh area, is situated in the southwest of Iran in the Zagros Mountains, which includes the High Zagros (HZ) and the Zagros Fold Belt (ZBF) (Fig. 1a).

Paleozoic rocks in the HZ are located in the higher and upper parts of the Zagros Mountains (with an altitude of up to about 3,000 meters) along the Zagros main fault. This tectonic zone has an NW-SE trend that is recognized as a narrow-thrust belt with a width of up to 80 km. One of the characteristics of this zone is the occurrence of the overthrust of anticlines exposing deep sedimentary rock units (Mesozoic and Paleozoic formations), the result of its intense tectonic deformation, uplift, and erosion. The ZFB is primarily composed of Tertiary rocks, with outcrops of Paleogene and Neogene rocks to the south of the Cretaceous and Paleogene rocks, respectively. (e.g., Berberian 1995).

In the Qalikuh area (Fig. 1a), differential uplift during the Zagros Orogeny meant that geological units including the Sargelu and Garau Formations were less deeply buried than in other parts of the Zagros fold-and-thrust belt. As a result, the thermal maturity of these formation is lower in this area than it is elsewhere. The lithostratigraphy of the Qalikuh area has been shown in Fig. 1c. The Middle Jurassic succession in the Qalikuh area begins with the deposition of the carbonates of the Surmeh Formation (49-136 m thick) which is conformably covered by the Middle Jurassic Sargelu Formation.

Previous studies (Shekarifard et al. 2019; Rasouli et al. 2015) have shown that the Sargelu and Garau formations in the Qalikuh area have the characteristics of oil shales, with very high TOC contents and low thermal maturity. Sargelu Formation is dominated by argillaceous limestones, interpreted to have been deposited in deep marine conditions with localized anoxia (Motiei 1993). Organic-rich strata in the Sargelu shales are frequently isolated by thick evaporitic intervals (Bordenave and Burwood 1990). The Sargelu Formation disconformably overlies the Najmeh Formation. At the Qalikuh area, the Sargelu Formation, with a thickness of 35-108 m, comprises thin-bedded, black bituminous, and dolomitic limestones with thin chert layers. The fauna of the formation is characterized by Posidonia. In this area, the Sargelu Formation is unconformably overlain by the Upper Jurassic Najmah Formation. The Najmah Formation is disconformably overlain by the salty-limestone Gotnia Formation (Fig. 1c and d). In the Qalikuh area, the Lower Cretaceous Garau Formation rests unconformably on the Gotnia Formation (Fig. 1c-d) and begins with 2-3 m of thin-bedded limestones which are overlain by black oil shales. The Garau Formation is overlain by conglomerates equivalent to the Bakhtiari Formation (Pliocene-Pleistocene) and by Quaternary alluvium.

Oil shale sampling and methods

The Sargelu oil shale was sampled from surface outcrop sections in the Qalikuh area (Fig. 1a-b). For this purpose, a total of 50 samples from the Sargelu oil shale, having a vertical sampling distance of 1-1.5 m, from eight different adopted outcrops were systematically collected (Fig. 1b and 2). The Sargelu oil shale in the Qalikuh area, is distinguished by significant lateral variations in thickness from 3 m thick individual beds up to 40 m thick units (mean: 28 m), and are easily distinguishable in the field from the adjacent rock units (Figs 1d and 3a). Petrographic observations on thin sections from the Sargelu oil shale are closely similar to those from the Garau oil shale, and show the presence of abundant organic matter with calcite crystals (Fig. 3b).

Table 1 summarizes the samples of the Sargelu oil shale collected, the analytical approaches used, and the number of samples examined for each method.

Rock-Eval pyrolysis and TOC analysis

A Rock-Eval VI pyrolysis apparatus was used to characterize the bulk geochemical properties of the Sargelu oil shale (Behar et al. 2001). The TOC content of the oil shale samples was determined using a Leco instrument. Table 1 provides the results of the TOC and Rock-Eval VI data for the Sargelu oil shale.

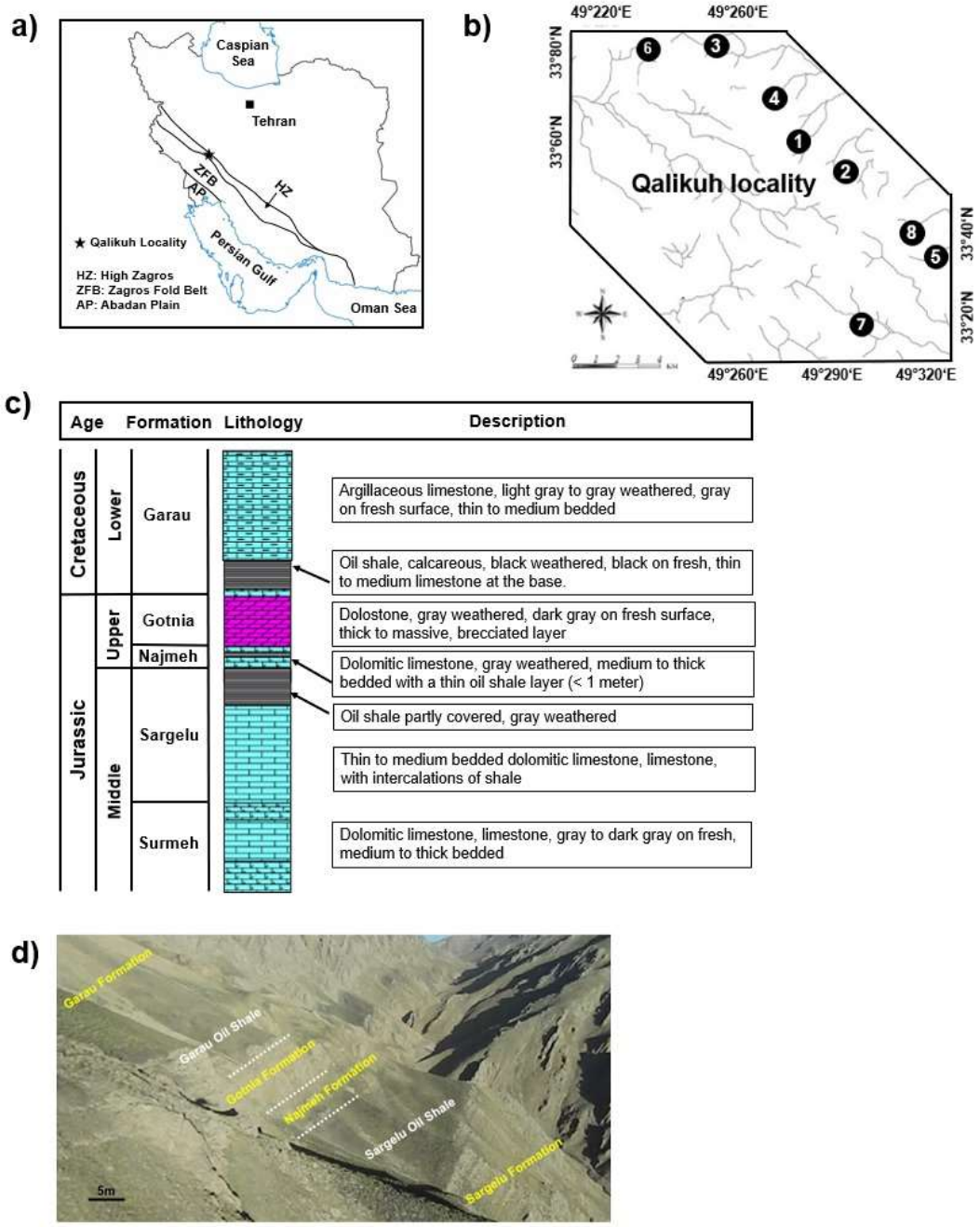

Figure 1. (a) The Qalikuh area in the High Zagros from the Zagros Mountains, SW Iran; (b) The studied surface outcrop sections (1 - 8) from the Sargelu and Garau oil shale at the Qalikuh area, (c) The local stratigraphy and lithological units underlying and overlying the Qalikuh oil shales; and (d) General view of the main lithostratigraphy units and the oil shales investigated

Table 1. The results of TOC and Rock-Eval VI pyrolysis analysis from the Sargelu oil shale in the Qalikuh area along with the selected samples for advanced (follow up) geochemical analyses

	Sample ID		Rock-Eval VI pyrolysis							
Region	(follow up analysis)	TOC (wt%)	S_1 (mg/g)	S_2 (mg/g)	GP	S_3 (mg/g)	T_{max} (°C)	HI	OI	PI
Location 1	SH 25	21.40	4.71	117.78	122.50	1.01	433	550	5	0.04
	SH 27	16.80	0.76	100.09	100.80	1.14	437	596	7	0.01
	GH 29 (f)	20.46	1.40	93.33	94.73	2.56	438	456	13	0.01
Location 2	GH 5	11.40	0.56	57.16	57.70	1.30	435	501	11	0.01
	GH 7	7.60	0.41	45.44	45.80	1.03	432	598	14	0.01
	GH 8	13.10	1.74	66.80	68.50	1.20	430	510	9	0.03
	GH 10	3.87	0.07	31.17	31.20	0.35	439	805	9	0.00
Location 3	GH 188	13.20	2.00	70.59	72.60	1.01	436	535	8	0.03
	GH 189	14.60	2.99	81.84	84.80	1.00	436	561	7	0.04
	GH 190	23.70	7.48	145.25	152.70	1.14	436	613	5	0.05
	GH 191	19.60	4.44	111.34	115.80	1.27	432	568	6	0.04
	GH 192	20.90	6.08	125.51	131.60	0.84	436	601	4	0.05
	GH 193	10.90	1.21	60.88	62.10	1.11	434	559	10	0.02
	GH 194	10.50	1.62	64.39	66.00	1.33	434	613	13	0.02
	GH 195	11.80	1.05	66.96	68.00	1.39	434	567	12	0.02
	SH 11	11.20	0.58	55.52	56.10	2.88	431	496	26	0.01
	SH 12	7.02	1.98	48.63	50.60	0.44	434	693	6	0.04
	SH 14	8.56	2.67	53.71	56.40	0.66	430	627	8	0.05
	SH 16 (a-g)	23.30	5.99	142.95	148.90	0.71	437	614	3	0.04
	SH 17	18.60	2.16	105.86	108.00	2.58	434	569	14	0.02
	SH 18	24.20	3.47	120.69	124.20	3.15	431	499	13	0.03
	SH 19	22.80	3.64	135.76	139.40	0.95	437	595	4	0.03
	SH 20	14.10	1.79	82.42	84.20	0.84	436	585	6	0.02
	SH 21	12.60	1.43	70.50	71.90	1.12	439	560	9	0.02
Location 4	MZY 4102	5.31	0.17	26.77	26.90	1.28	434	504	24	0.01
	MZY 4102	4.88	0.19	27.07	27.30	1.19	436	555	24	0.01
	MZY 4121	12.20	0.40	63.95	64.30	1.94	434	524	16	0.01
	MZY 4122	20.20	2.60	111.49	114.10	1.37	433	552	7	0.02
	MZY 4123 (a-g)	22.40	2.99	128.31	131.30	1.63	436	573	7	0.02
Location 5	GH 127	15.30	1.07	75.25	76.30	0.91	435	492	6	0.01
	GH 128	8.78	0.60	47.14	47.70	0.93	435	537	11	0.01
	GH 129	13.80	1.00	72.98	74.00	1.27	431	529	9	0.01
Location 6	GH 166	12.80	1.09	58.49	59.60	2.82	423	457	22	0.02
	GH 168	17.30	1.19	91.30	92.50	1.97	436	528	11	0.01
	GH 170	20.60	2.55	100.49	103.00	3.32	429	488	16	0.02
	GH 172	17.90	2.32	92.25	94.60	2.05	432	515	11	0.02
	GH 174	14.60	1.28	69.37	70.70	2.33	428	475	16	0.02
	GH 176 (a-c)	22.50	3.40	117.62	121.00	2.82	427	523	13	0.03
	GH 178	16.80	1.53	81.84	83.40	1.97	430	487	12	0.02
	GH 180	19.00	2.45	99.33	101.80	1.58	430	523	8	0.02
	GH 183	17.80	2.27	88.95	91.20	2.66	428	500	15	0.02
	MZY 4160	22.00	2.88	125.28	128.20	2.89	429	569	13	0.02
	MZY 4161	17.30	2.16	98.74	100.90	2.19	430	571	13	0.02
	MZY 4163	22.70	3.01	117.81	120.80	2.35	428	519	10	0.02
Location 7	90GH 31	13.00	0.77	59.78	60.50	1.63	434	460	13	0.01
	90GH 36	19.40	2.03	115.55	117.60	1.19	435	596	6	0.02
Location 8	MZY 3983	9.45	0.40	42.97	43.37	1.32	433	455	14	0.01
	MZY 3984 (a-c)	16.30	1.20	89.32	90.52	2.19	432	548	13	0.01
	MZY 4000	7.60	0.34	39.92	40.26	1.68	434	525	22	0.01
	MZY 4001	21.40	1.94	111.64	113.60	3.41	432	522	16	0.02

(a): elemental analysis of kerogen; (b): organic petrography and VK analysis; (c): vitrinite reflectance (VRr); (d): XRF and XRD analysis; (e): GC and GC-MS analysis; (f): Pyrolysis-GC analysis; (g): carbon isotope analysis.

TOC (Total organic carbon): weight %
S_1: mg hydrocarbon / g rock
S_2: mg hydrocarbon / g rock
S_3: mg CO_2 / g rock
T_{max} (Maximum temperature): ºC
PI (Production index): S_1 / (S_1+S_2)
GP (Genetic potential): S_1 + S_2
GC: gas chromatography
GC-MS: gas chromatography-mass spectrometry
Pyrolysis-GC: Pyrolysis-gas chromatography
XRD: X-ray diffractometer
XRF: X-ray Fluorescence

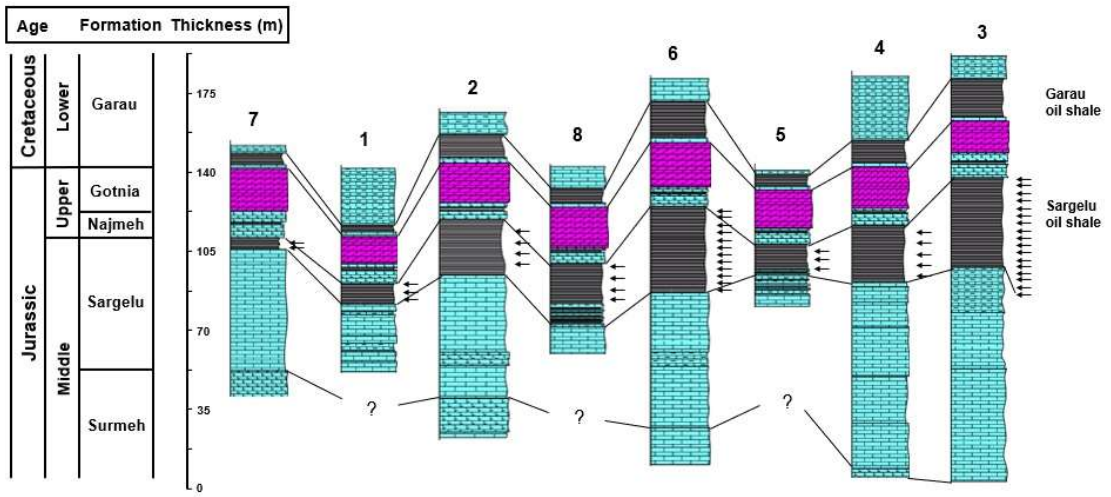

Figure 2. Lithostratigraphy and lateral correlation of the Sargelu and Garau oil shales with the underlying and overlying geological formations in the sections investigated in the Qalikuh area from the Zagros Mountains, SW Iran. Refer to Figure 1c for description of the geological formations. Numbers point out the investigated outcrop sections in Figure 1b. Arrows show the position of the Sargelu oil shale sampling

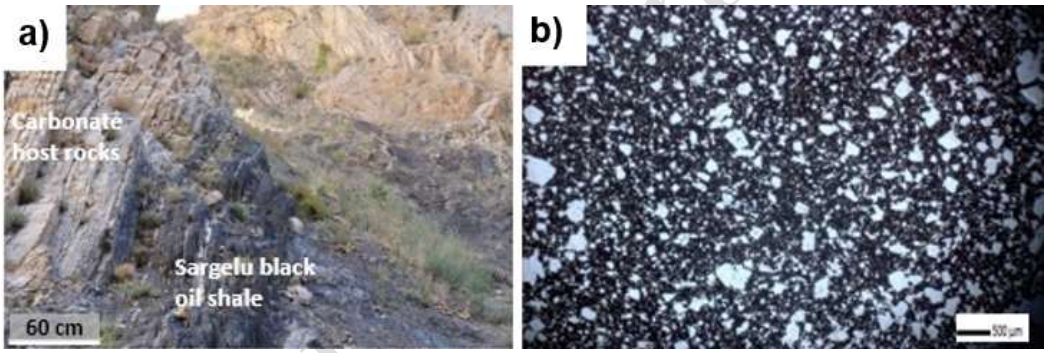

Figure 3. (a) Sharp contact of the Sargelu black oil shale with the carbonate host rocks from the Qalikuh area in the Zagros Mountains; (b) Thin section photomicrograph of an oil shale sample, where two major components are observed with bitumen and white calcite crystals (transmitted light)

Pyrolysis-gas chromatography (GC) analysis

The selected Sargelu oil shale samples (Table 1) were investigated by applying the open Pyrolysis-GC technique and then GCs were employed to illustrate the results while focusing on n-C_{10} and n-C_{14} components. The relative abundance of gaseous and light hydrocarbons (HCs) was compared with n-C_{14}+ components to evaluate product types. For additional characterization of the kerogen quality and pyrolysate composition (gas-oil ratio), Pyrolysis-GC was applied only to representative sample GH 29 (Table 2). For open Pyrolysis -GC, a micro-scale sealed-vessel pyrolysis injector system connected to an Agilent GC-6890A was used to test 30 mg of the sample (Horsfield 1989).

Elemental analysis

A Thermo Scientific Flash EA 1112 Thermo elemental analyzer was utilized for the elemental analysis of four kerogens. Furthermore, the content of C, H, N, S, Fe and O elements was determined in two separate experiments (Table 3).

Table 2. Open pyrolysis-GC normalized single compound yields from the selected Sargelu oil shale (sample GH 29) as input parameters for determination of kerogen quality and structure using ternary diagrams of Horsfield (1989), Larter (1984), and Eglinton et al. (1990)

Horsfield (1989) chain length distribution			GOR	Larter (1984) terrestrial input			Eglinton et al. (1990) marine input		
Total C_{1-5}	C_{6-14}	C_{15}^{+}	C_{1-5}/C_{6+}	Phenol	m, p-Xylene	n-$C_{8:1}$	o-Xylene	2,3-DM-Thiophen	n-$C_{9:1}$
80	17	3	4	0	37	63	28	6	66

GOR = Gas oil ratio (kg/kg),

Table 3. (a) Results of elemental analysis of kerogen, (b) Bitumen reflectance (BRr) measurement and equivalent vitrinite reflectance (VRr) calculated and (c) X-ray Fluorescence (XRF) results for the selected Sargelu oil shale samples

(a)

Sample ID	% C	% H	% N	% O	% S	% Fe	H/C ratio	O/C ratio	S/C ratio	N/C ratio
GH 176	64.00	6.00	0.90	4.30	9.80	0.40	1.13	0.05	0.11	0.01
SH 16	55.20	5.50	0.90	2.80	9.90	2.30	1.20	0.04	0.13	0.01
MZY 4123	53.00	5.10	1.00	2.80	9.40	2.00	1.15	0.04	0.13	0.01
MZY 3984	69.50	6.50	1.00	2.20	10.60	0.50	1.12	0.02	0.11	0.02

(b)

Sample ID	No. of measurements	Arithmetic Mean (BRr %)	Standard Deviation	Equivalent VRr %
GH 176	28	0.48	0.04	0.69
SH 16	20	0.40	0.05	0.61
MZY 4123	21	0.40	0.07	0.61
MZY 3984	21	0.45	0.04	0.66

(c)

Sample ID	MgO (%)	Al_2O_3 (%)	SiO_2 (%)	P_2O_5 (%)	SO_3 (%)	K_2O (%)	CaO (%)	TiO_2 (%)	Fe_2O_3 (%)	NiO (%)	V_2O_5 (%)	MoO_3 (%)	CuO (ppm)
SH 16	0.97	5.60	17.61	0.55	16.76	1.76	49.35	0.54	3.71	n.d	0.88	n.d	n.d
MZY 4123	1.18	5.08	16.12	0.14	16.04	1.85	52.27	0.44	3.30	n.d	1.45	n.d	965

n.d: not determined

Kerogen petrography and bitumen reflectance measurements

In this research, four samples were selected for visual kerogen (VK) analysis and organic petrography (Table 1), and transmitted light microscopy was used for qualitative VK observations**.** Reflected white and UV light microscopy (with a Zeiss UMSP 50) were utilized for conducting kerogen petrography on the polished blocks of the bulk samples. Due to the absence of vitrinite macerals, the reflectance of bitumen (BRr) analysis was conducted on the samples (Taylor et al., 1998). Table 3b presents the results of reflectance measurements on bitumen.

X-ray fluorescence (XRF) and X-ray diffractometer (XRD) analyses

To characterize the chemical composition and the mineralogy of the Sargelu oil shale, two samples were investigated by XRF and XRD, respectively. Table 3c lists the results of the XRF analysis.

Solvent extraction and geochemistry

The free hydrocarbons were extracted from the chosen oil shale samples by employing the

solvent extraction method. This solvent consisted of DCM/methanol (MeOH) 93/7% vol using a Soxhlet-type system. Next, the elemental sulfur was removed by adding activated copper. The samples were then extracted for 24 hours, followed by centrifuging the prepared solution. Liquid column chromatography was used for separating the extracts into nitrogen/sulfur/oxygen (NSO) compounds, saturated HCs, and aromatic HCs.

The selected samples were analyzed by the GC-flame ionization detector (FID) by applying various approaches for aromatic and saturated HC fractions, including a Hewlett Packard 5890 Series II Gas Chromatograph with the incorporation of an FID. Moreover, an MD800 series GC-mass spectrometry was utilized in this regard. Also, the mass spectrometer was directly connected to an Agilent 6890 series, and Mass Lynx software was used to run the system**.** The bulk isotopic was analyzed using a VG 602 Dual Inlet Isotope Ratio Mass Spectrometer on isolated kerogens of saturated and aromatic HCs. The results of the conducted analyses on the extracts are provided in Table 4.

Results and discussion

TOC richness and Rock-Eval data

The TOC is considered a fundamental factor for evaluating petroleum SRs and oil shale resources. This assessment is usually conducted by utilizing a carbon analyzer (e.g., Hunt 1996). Based on the obtained results, the TOC content of the Sargelu oil shale from the Qalikuh area ranges from 3.87 to 24.2 wt% (mean: 15.47 wt%). Accordingly, the Sargelu oil shale, similar to the Garau oil shale, contains extremely high amounts of organic carbon.

Table 4. (a) Bulk properties of solvent extracts composition, GC parameters and carbon isotope values; (b) source dependent; and (c) maturity-dependent biomarker parameters from the selected Sargelu oil shale samples

(a)

Sample ID	% Sat	% Aro	% NSO	Pr/Ph	Pr/C_{17}	Ph/C_{18}	CPI	$\delta^{13}C_{sat}$	$\delta^{13}C_{aro}$	$\delta^{13}C_{kerogen}$
SH10	10.13	43.20	46.67	0.90	0.36	0.39	0.48	-27,37	-27,91	-27.67
MZY 4123	7.29	38.08	54.63	0.97	0.33	0.37	0.48	-26,99	-28,11	-28.24

(b)

Sample ID	DBT/Phen	$C_{31}R/C_{30}$ Hopane	C_{29}/C_{30} Hopane	Gammacerane/ Hopane C_{30}
SH10	4.90	0.41	2.56	0.06
MZY 4123	5.36	0.45	2.38	0.08

	% C_{27} Sterane	% C_{28} Sterane	% C_{29} Sterane	C_{27}/C_{29} Sterane	Sterane/ Hopane
SH10	30.21	24.38	45.44	0.67	0.19
MZY 4123	29.48	25.51	45.02	0.65	0.14

(c)

Sample ID	Ts/Tm	22S/(22S+22R) C_{32} Hopane	20S/(20S+20R) C_{29} Sterane	MPI-1	4-MDBT/ 1-MDBT
SH10	0.026	0.57	0.51	0.68	1.12
MZY 4123	0.028	0.59	0.51	0.68	1.23

Sat= Saturate, Aro= Aromatic, NSO= Heteroatoms, Asp= Asphaltene, Pr/Ph = pristane/phytane ratio, CPI=Carbon Preference Index, %C_{27} = %C_{27}ααα R-/C_{27}–C_{29}ααα R-steranes, %C_{28} = %C_{28}ααα R-/C_{27}–C_{29}ααα R-steranes, %C_{29} = %C_{29}ααα R-/C_{27}–C_{29}ααα R-steranes, DBT/Phen= Dibenzothiophene/ Phenanthrene, Ts=18α(H)-22,29,30-trinsnorneohopane, Tm=17α(H)-22,29,30-trisnorhopane, MPI-1=Methyl Phenanthrene Index, MDBT=Methyldibenzothiophene.

According to the Rock-Eval pyrolysis data, the mean hydrogen index (HI) value of the Sargelu oil shale is 548 mg HC/g TOC (in the range of 455-805 mg HC/g TOC). The remaining potential (S_2) for the samples reaches up to 145.25 mg HC/g rock (mean: 84.16 mg HC/g rock). These parameters reflect superior capability for oil generation. A cross-plot of HI versus OI plot shows Type I kerogen although most examined samples are acknowledged as Type II kerogen based on the HI-T_{max} plot (Fig. 4a-b), indicating that the Type II-S kerogen on the HI-OI plot can indicate the position of Type l Kerogen.

As indicated in Table 5, the Sargelu oil shale, similar to the Garau oil shale, has a maturity just at the beginning of the oil window or slightly less than that based on the mean value of T_{max} (433°C), production index (PI), and S_1/TOC ratio (mean: 0.11). The high level of petroleum compounds in the oil shale (high S_2 and HI values) with the existence of Type II-S kerogen (Section 5.3) is considered the primary cause of the low mean of T_{max}, namely, as high as 433°C (cf. Tissot et al. 1987). The S_2 versus TOC plot indicates the occurrence of Type II kerogen in the Sargelu oil shale and an excellent agreement between S_2 and TOC values (Fig. 5).

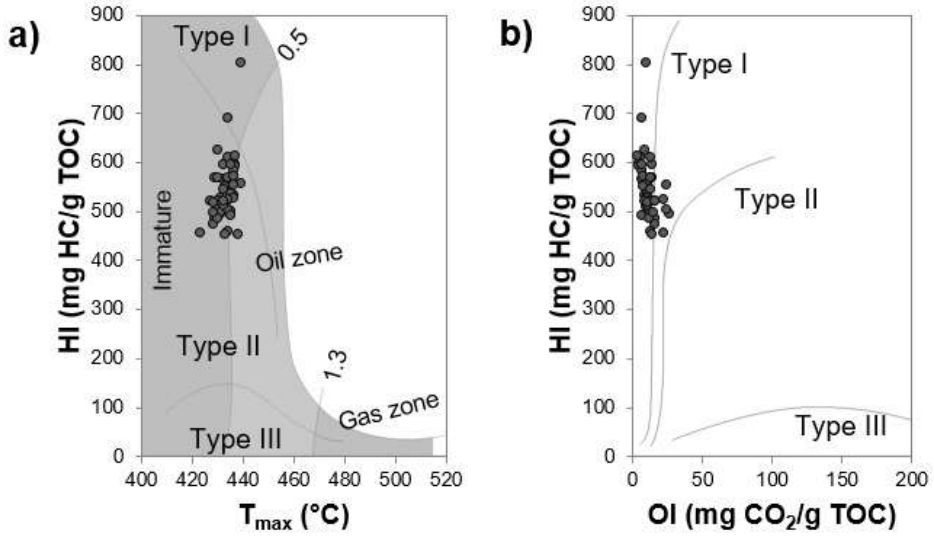

Figure 4. Quality, thermal maturity status and kerogen type of the studied Sargelu oil shale represented by (a) the relationship between hydrogen index (HI) and apex of the S_2 peak (Tmax), and (b) the relationship between hydrogen index (HI) and oxygen index (OI). Note that 50-60% of the kerogen is convertible to oil and gas

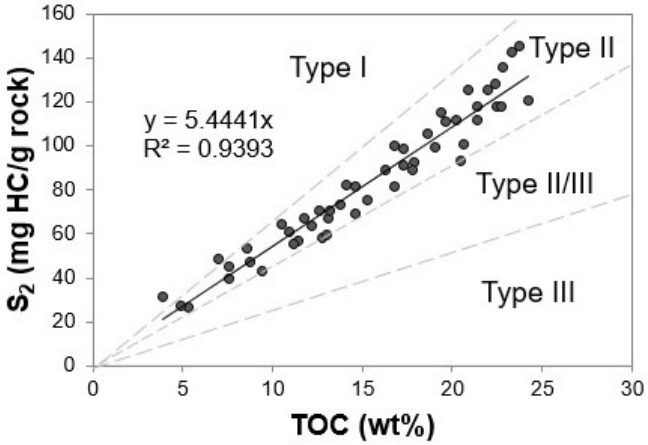

Figure 5. Occurrence of Type II kerogen and very good correlation between petroleum generation potential (S_2) and total organic carbon (TOC) for the Sargelu oil shale, Qalikuh area. TOC values can be used as a proxy to evaluate the petroleum potential of the Sargelu oil shale

The genetic capability (S_1+S_2) related to the calculated values of the Sargelu samples ranges from 26.9 to 152.7 mg HC/g rock (mean: 86.2 mg HC/g rock), demonstrating overall high to extremely high oil capability. The values of the genetic potential for the Sargelu oil shale have proven to be in close correlation with TOC values. According to HI and TOC values and the S_2/S_3 ratio, the Sargelu oil shale, similar to the Garau oil shale, has good to excellent capability for oil generation (Tissot and Welte 1984; Peters and Cassa 1994). Interestingly, the range and mean value of the Rock-Eval pyrolysis and TOC data from the Sargelu oil shale are highly similar to those of the Garau oil shale (Table 5) from the Qalikuh area in the Zagros Mountains.

Pyrolysates composition

The acquired gas chromatograms by Pyrolysis -GC from the three oil shale samples (Table 1) yielded the same pattern, indicating that most likely, all samples have the identical capacity to generate close products after being fully matured and heated.

The outstanding potential of the Sargelu oil shale for generating predominately gaseous and light liquid HCs with insignificant levels of n-C_{14}+ heavy HCs has been confirmed by pyrolysis products (Fig. 6). The general relative peak pattern and the pattern of pyrolysis products for the Pyrolysis -GC chromatograms from the Sargelu oil shale are extremely similar to those from the Garau oil shale (Shekarifard et al. 2019). According to the results of the pyrolysate composition from the sample GH 29, the type of the generated petroleum during the full maturation of the Sargelu oil shale is expected to be rich in gas (total $C_{1\text{-}5}$: 80%, $C_{6\text{–}14}$: 17%, Table 2). However, the HI value of 456 mg HC/g TOC and the S_2 value of 93.33 mg HC/g rock from this sample represent an oil-prone sample (Table 1). It is noteworthy that methane represents approximately 50% of the molecules at subsurface conditions, even in standard North Sea black oil (England et al. 1987). In high-quality SR-basins, the gas-to-oil ratio of oil fields is mostly caused by the properties of the cap rock and the loss of gas during migration, which is a result of the primary kerogen qualities (Sales 1997; England and Mackenzie 1989; Karlsen and Skeie 2006).

In the Horsfield ternary diagram (1989), pyrolysis sample plots are on the border of the gas-condensate field with the low wax paraffinic-naphthenic-aromatic (P-N-A) oil field. Due to the lack of phenol and the dominance of n-octene compounds in pyrolysate products (Table 2), the gas-condensate generation capacity of the sample is seemingly unrelated to the existence of the terrestrial OM input.

Table 5. Comparison of Rock-Eval VI data of the Sargelu and Garau oil shales in the Qalikuh area in the Zagros Mountains

Rock-Eval data	Sargelu oil shale (n=50)	Garau oil shale (n=123)
TOC (wt%)	3.87-24.20 (15.47)	3.83-26.40 (16.48)
T_{max} (°C)	423-439 (433)	423-441 (431)
HI (mg HC/g TOC)	455-805 (548)	329-743 (557)
OI (mg CO_2/g TOC)	3-26 (11.40)	2-56 (11)
S_1 (mg HC/g rock)	0.07-7.48 (2.05)	0.10-4.62 (1.83)
S_2 (mg HC/g rock)	26.77-145.20 (84.16)	1.17-140.20 (88.90)
S_3 (mg CO_2/g rock)	0.35-3.41 (1.64)	0.40-4.22 (1.51)
S_2/S_3	19.28-201.34 (62.37)	1.65-289.61 (75.01)
S_1/TOC	0.02-0.20 (0.11)	0.02-0.20 (0.10)
GP (S_1+S_2)	26.90-152.70 (86.20)	1.42-144.80 (90.70)
PI	0.00-0.05 (0.02)	0.00-0.18 (0.02)
Reference	This study	Shekarifard et al. 2019

n: number of investigated samples; range (mean)

This is supported by the organic petrography and geochemical evidence (refer to the next chapters). Thus, gas-light oil generative characteristics are simple and most probably owing to the primary algal-Type II-S kerogen composition (cf. Shekarifard et al. 2019).

The investigated Sargelu oil shale, similar to the Garau oil shale, evidently hosts excellent potential as a source for gas and light oil when obtaining the essential thermal maturity for the thermo-catalytic gas (more than 1.35% VRr). Therefore, the Sargelu oil shale can also be considered as excellent gas and light oil SRs in a petroleum system and/or a good shale oil or shale gas reservoir in an unconventional petroleum system.

Kerogen elemental composition

According to the elemental study of the selected kerogens (Table 3a), high levels of sulfur (S) from the kerogens are evident (9.4-10.6 wt%). This quantity of sulfur and the S/C ratio (mean: 0.12) signifies the existence of S-rich kerogen in the Sargelu oil shale (Table 6). The primary sulfur is incorporated into kerogen based on the low levels of iron (Fe) in the kerogens (mean: 1.3 wt%). The hydrogen (H) level of the kerogens has a range of 5.1-6.5 wt% (mean: 5.77 wt%), which is ample evidence of H-rich kerogens in the Sargelu samples (Hunt 1996). The Sargelu kerogens represent a higher amount of Fe, mainly due to a higher abundance of pyrite in comparison to the Garau kerogens. The kerogen data of the Sargelu and Garau oil shales are highly similar to each other except for Fe (Table 6).

The assessed atomic ratios of the kerogens for the H/C and O/C atomic ratios vary between 1.15 and 1.20, as well as 0.02 and 0.05, respectively (Table 3a). The van Krevelen plot suggests that the analyzed kerogens have entered the catagenesis window along the maturation route of Type I kerogen, which is the same position as the Garau oil shale kerogens (Fig. 7).

Kerogen typing by petrography

The VK analysis confirms that the OM in the Sargelu oil shale is nearly totally amorphous OM (AOM), similar to that in the Garau oil shale (Shekarifard et al. 2019).

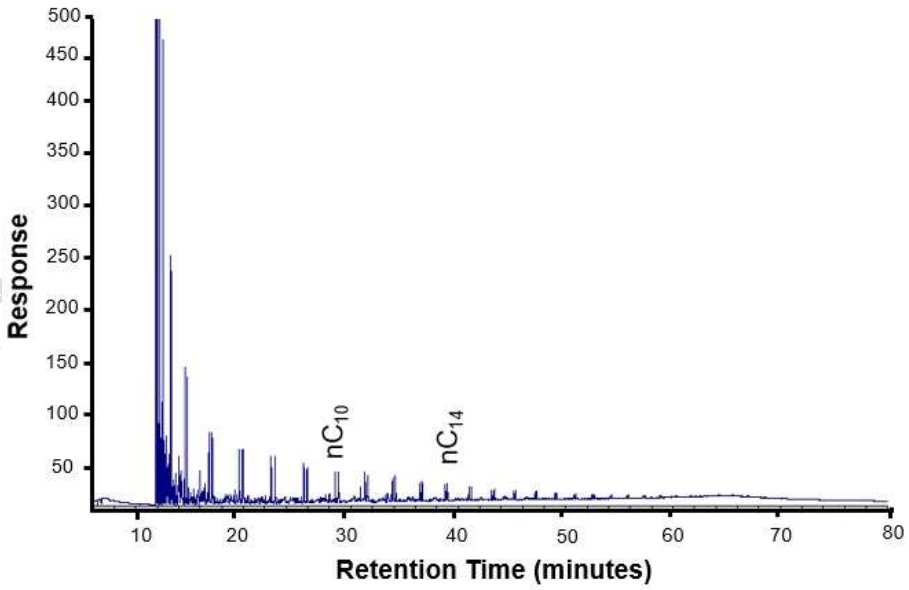

Figure 6. The gas chromatogram of the Pyrolysis -GC analysis of the representative sample SH 16, showing the pyrolysis products of the Sargelu oil shale. The dominance of gas and light oil is evident during the pyrolysis and artificial final maturation of the sample

Table 6. Comparison of the elemental analysis and chemical composition of the kerogen from the Sargelu and Garau oil shales at the Qalikuh area

Element	Sargelu oil shale (n=4)	Garau oil shale (n=4)
% C	53.00-69.50 (60.42)	52.70-73.40 (65.40)
% H	5.10-6.50 (5.77)	5.20-7.10 (6.20)
% N	0.90-1.00 (0.95)	0.90-1.00 (0.90)
% O	2.20-4.30 (3.02)	1.90-3.40 (2.90)
% S	9.80-10.60 (9.92)	9.00-12.10 (10.50)
% Fe	0.40-2.30 (1.30) ↑	0.08-2.30 (0.70) ↓
H/C ratio	1.12-1.20 (1.15)	1.12-1.16 (1.15)
O/C ratio	0.02-0.05 (0.04)	0.02-0.04 (0.03)
S/C ratio	0.11-0.13 (0.12)	0.15-0.23 (0.17)
N/C ratio	0.01-0.02 (0.01)	0.01-0.01 (0.01)
Reference	This study	Shekarifard et al. 2019

n: number of investigated samples; range (mean)

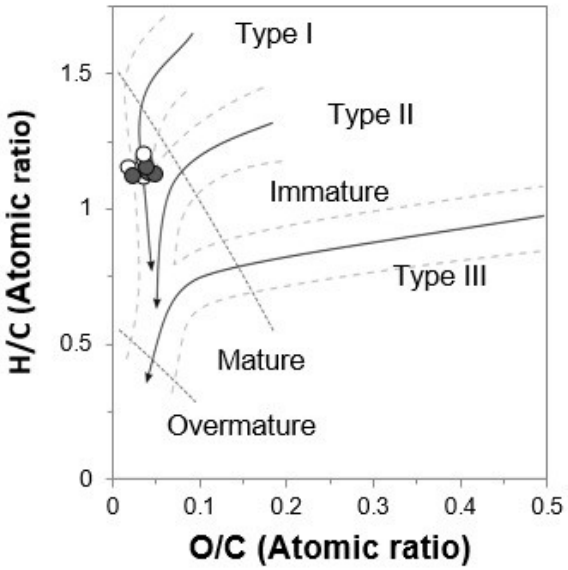

Figure 7. The Van Krevelen diagram for the examined kerogens indicating the beginning of catagenesis during thermal maturation of the Sargelu oil shale (black circles) and Garau oil shale (white circles) at the Qalikuh area. The data points of kerogens from the Sargelu and Garau oil shale show the same position on the plot, indicating the same level of maturity and the same chemical composition

Bitumen maceral is the primary and nearly the only organic element of the studied Sargelu oil shale. Its major occurrence is the pervasive impregnation, filling the pores and forming the matrix of the oil shale (Fig. 8a-b). A few small particles of inertinite are observed occasionally (Fig. 8b). Based on microscopic investigations, the euhedral calcite is the most identified mineral (Fig. 8a). Quality observations show more contributions of pyrite framboids in some investigated samples (Fig. 8b-c) compared to the Garau oil shale. According to microscopic observations, the occurrence of the two types of bitumen is similar to that of the Garau oil shale (Fig. 8c-d). The first type demonstrates higher bitumen reflectance without fluorescence, while the second one, with an insignificant generation, permeates pores and fractures with lower reflectance and bright yellow fluorescence (Fig. 8d). The latter type suggests the initial stage of oil generation from the Sargelu oil shale (Taylor et al. 1998; Stasiuk et al. 2006).

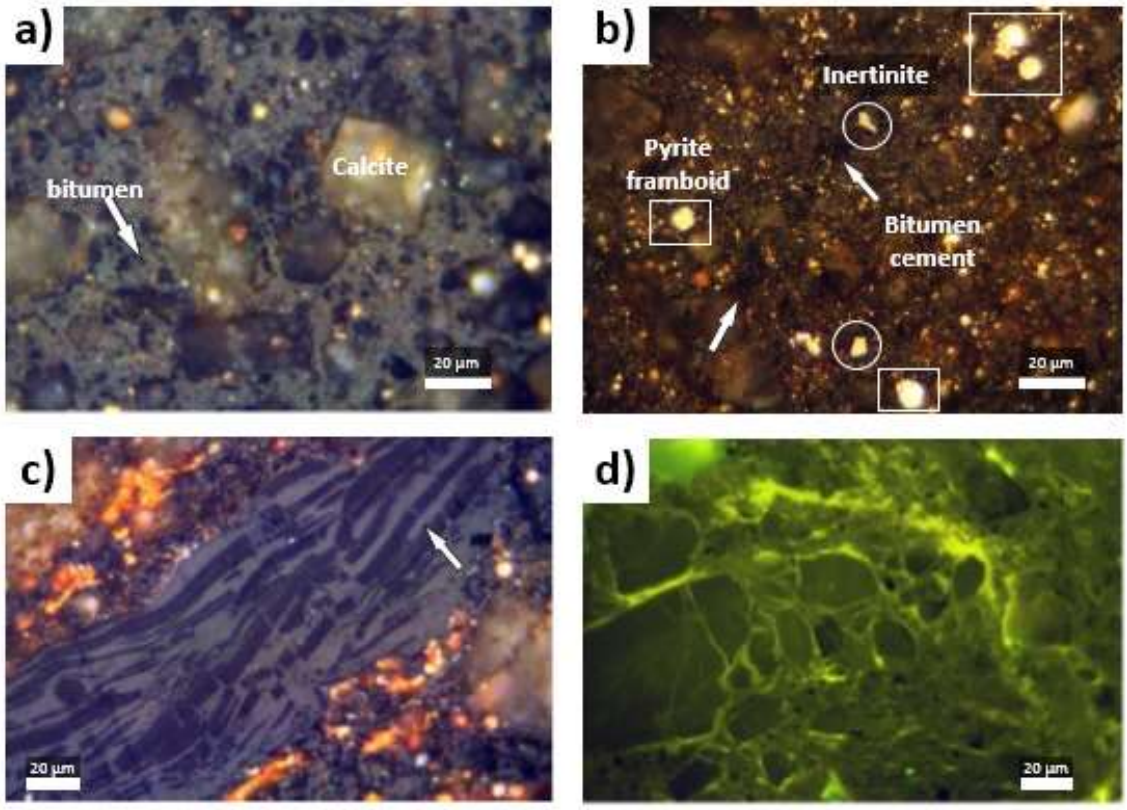

Figure 8. Photomicrographs of kerogen from the Sargelu oil shale under reflected light; (a) Oil shale with calcite crystals, cemented by bitumen (VRr: 0.5-0.6%; Plane polarized light, oil immersion, width 200 µm); (b) Compared to other investigated samples, the bitumen cement is less evident, arrow: bitumen cement, circles: inertinite, rectangle: pyrite framboids (Plane polarized light, oil immersion, width 200 µm); (c) Two generation of bitumen in a vein (arrow), spreading laterally as a cement to minerals with many pyrites which were altered as iron oxides-hydroxides (crossed polar, oil immersion, width 200 µm); (d) A thin late fluorescence bitumen film occurs as veinlets and interstitial to mineral grains (UV light, oil immersion, width 200 µm)

Mineralogy and chemical composition

The XRD study results proved that calcite, with some minor amounts of quartz, pyrite, and feldspar, is the main mineral of the Sargelu oil shale. Furthermore, the XRF analysis revealed that calcite is the main mineral in the evaluated samples (mean CaO: 50.81 wt%). The SiO_2 content of the samples is between 16.12 and 17.62 wt%, signifying the existence of silica or quartz**.** The mass concentration of SO_3 for the studied samples is between 16.03 and 16.77 wt% while varying from 3.30 to 3.71 wt% for Fe_2O_3. This data indicates the existence of sulfur and some pyrites in the samples.

Although the low content of Al_2O_3 (mean: 5.34 wt%) suggests limited amounts of clay minerals, the Sargelu oil shale shows a more argillaceous character as opposed to the Garau oil shale (mean Al_2O_3: 2.35 wt%). Furthermore, the lower CaO content leads to higher amounts of K_2O, and the higher content of SiO_2 detected from the Sargelu oil shale is consistent with the more clayey nature of the Sargelu oil shale (Table 7). Compared to the Garau oil shale, the Sargelu oil shale is enhanced in vanadium (Table 7). It seems the Sargelu oil shale was deposited farther from the beach and experienced a deeper marine environment in comparison to the Garau oil shale.

Table 7. Comparison of the sXRF results of the Sargelu and Garau oil shales in the Qalikuh area of the Zagros Mountains

	MgO (%)	Al_2O_3 (%)	SiO_2 (%)	P_2O_5 (%)	SO_3 (%)	K_2O (%)	CaO (%)	TiO_2 (%)	Fe_2O_3 (%)	NiO (%)	V_2O_5 (%)	MoO_3 (%)	CuO (ppm)
Sargelu oil shale (n=2)	1.07	5.34 ↑	16.86	0.34	16.40	1.8	50.81↓	0.49	3.50	n.d	1.16↑	n.d	n.d
Garau oil shale (n=3)	0.71	2.35 ↓	10.24	0.51	14.96	0.93	67.10↑	0.37	2.62	0.12	0.51↓	0.21	407

n: number of investigated samples; data is mean value; n.d: not determined

Geochemical characterization of the extracts

Extracts composition

The dominance of the non-HCs (46.67-54.63% NSO components), 38.08-43.20% of aromatic HCs, and 7.29-10.13% of saturated HCs is evident based on the composition of the Sargelu oil shale extracts (Table 4a). The low fraction of saturated HCs is in notable opposition to the great enrichment in non-HCs (up to 54.63%). The Sargelu oil shale extracts demonstrate higher contents of aromatic HCs and lower amounts of NSO components compared to the Garau oil shale extracts (Table 8). Similar to the Garau oil shale extracts, the chemical composition of the Sargelu oil shale extracts is naphthenic (Tissot and Welte 1984).

n-alkanes and isoprenoids

The gas chromatogram in Fig. 9 displays the extracted saturated HCs of the two examined samples (SH 16 and MZY 4123) from the Sargelu oil shale. As shown, a clear bimodal distribution of low-moderate molecular weight n-alkanes, isoalkanes, and cycloalkanes (i.e., first population) and a second biomarker-hump is detectable. The overall pattern of the n-alkanes (first population) depicts a bell-shaped distribution. Based on this pattern, the samples are marginally mature, although biomarkers are still present. This distribution pattern (i.e., high contribution of biomarkers) and a clear bimodal pattern are the main differences between the GC extracts of the Sargelu and Garau oil shales (Shekarifard et al. 2019).

The presence of n-alkanes with low-moderate molecular weight, as well as the extremely low ratio of sterane/hopane (0.14-0.19, Table 4b), suggests that OM originates from marine organisms with high biodegradation during OM diagenesis**.** In the investigated oil shale, the pristane (Pr) and phytane (Ph) ratios have values less than 1 (Table 4a), implying anoxic conditions throughout the sedimentation of the Sargelu oil shale (e.g., Didyk et al. 1978; Montero-Serrano et al. 2010; Peters and Moldowan 1993). Furthermore, the appearance of pyrite framboids strengthens the existence of anoxic/euxinic conditions. Similar to the Garau oil shale, the analyzed extracts from the Sargelu exhibit a dominance of n-C_{17} and n-C_{18} over pristane and phytane, respectively. This observation indicates HC generation due to early-moderate thermal maturity (Table 4a). According to Pr/n-C_{17} and Ph/n-C_{18} ratios, Type II kerogen is the primary source of Sargelu extracts (Peters et al. 2008).

Terpenes

The studied Sargelu oil shale extracts demonstrate nearly identical patterns of the distribution of m/z 191 triterpenes and m/z 217 normal steranes. These patterns signify uniform OM sources and paleo-depositional circumstances throughout the deposition of the Sargelu oil shale. Fig. 9 illustrates the mass fragmentogram of the extracted saturated hydrocarbon fraction for the examined samples**.**

Similar to the Garau oil shale, the extracts from the Sargelu oil shale manifest a predominance

of Tm over Ts (Table 4c). This ratio for the Sargelu oil shale is similar to that of the Garau oil shale, both presenting an abnormally low level of maturation (mean: 0.027, Table 4c) while not displaying the anticipated level of maturation. This phenomenon likely depends on the depositional conditions (Moldowan and Fago 1986; Seifert and Moldowan 1978). The Ts/Tm ratio (0.5) increases with the portion of the shale in calcareous facies (Hunt 1996).

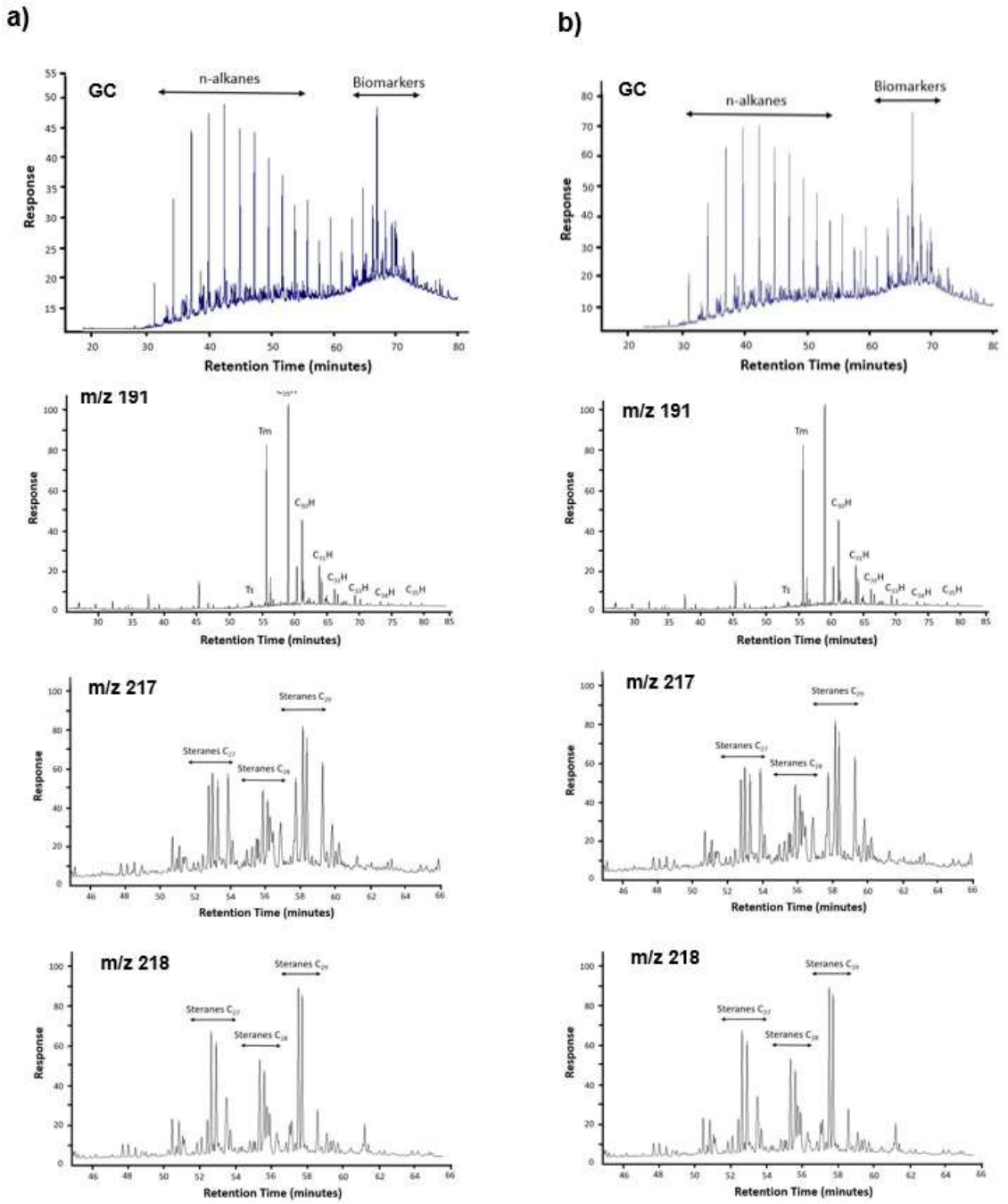

Figure 9. The gas chromatograms (GC), m/z 191 mass fragmentograms, m/z 217 mass fragmentograms, and m/z 218 mass fragmentograms of the extracted saturated hydrocarbon fraction for the sample SH 16 (a) and sample MZY 4123 (b) as the representatives for the Sargelu oil shale. Note the chromatograms for the samples are very similar and also note low amounts of tricyclic terpanes, and the dominance of C_{29} steranes, with – apparently low amounts of C_{30} steranes and little in terms of diasteranes

Although the abundance of C_{29}-norhopane is greater than the relative abundance of C_{30}-hopane in the Sargelu oil shale (Table 4b), the ratio is slightly less than that of the Garau oil shale (Table 8). The predominance of C_{29}-norhopane is related to carbonate-rich SRs, which is in agreement with the perceived and calculated mineralogy of the oil shales and other geochemical information (e.g., low sterane/hopane ratios, low contents of diasteranes, and the occurrence of tetracyclic terpanes). However, a lower ratio of C_{29}/C_{30} hopane for the Sargelu oil shale is associated with the lower levels of carbonates in the Sargelu oil shale. The Sargelu carbonate oil shale reflects possibly somewhat more argillaceous properties compared to the Garau oil shale. This character is also confirmed by petrography and XRF evidence. Further, the ratio of dibenzothiophene to phenanthrene (DBT/Phen) for the Sargelu oil shale extracts ranges from 4.90 to 5.36 (Table 4b), which is higher than that of the Garau oil shale (Table 8). This parameter supports the idea that the Sargelu oil shale formed in a mostly marine carbonate environment with less oxygen and more bacteria than the Garau oil shale.

For the studied extracts, comparatively high amounts of $C_{31}R/C_{30}$ hopane (0.41-0.45, Table 4b) imply a marine SR. According to Peters et al. (2005), the oil and extracts from marine SRs commonly exhibit high $C_{31}R/C_{30}$ hopane ratios (i.e., $C_{31}R/C_{30}$ >0.25). For the examined samples, the gammacerane/C_{30} hopane ratio is extensively low (<0.08), reflecting normal seawater throughout the sedimentation of the Sargelu oil shale (Table 4b).

Steranes

The pattern of the normal steranes of the m/z of 218 does not demonstrate a divergence between the Sargelu samples, nor are other biomarker parameters significantly different. The usual steranes of the Sargelu samples include $C_{29}>C_{27}>C_{28}$ (Table 4b), which is inconsistent with the trend of the obtained steranes from the Garau oil shale extracts (Table 8). Fig. 9 displays the distribution pattern of related m/z 218 mass fragmentograms for the two evaluated samples.

According to recent research, the C_{29}-sterols (steranes) exist in various microalgae, including freshwater eustigmatophytes and diatoms (Riboulleau et al. 2007). Furthermore, their main sources are nonmarine algae and bacteria (Moldowan et al. 1985). However, it was previously deemed that the C_{29}-sterols (steranes) dominate in land plants, and marine plankton is the primary source of C_{27}-sterols (Huang and Meinschein 1979). In addition, more pioneering studies confirm the predominance of C_{29}-steranes for most marine sediments. These sediments include pelagic sediments that are deposited extensively far from the terrestrial OM input (e.g., Volkman et al. 1983). Nonetheless, the dominance of C_{29} steranes is common in Paleozoic oils, which pre-dates land plants, and the origin of the steranes must be related to green algae, which are the precursors of land plants (Kodner et al. 2008).

As previously explained, the OM is totally constituted of AOM in kerogen petrography. According to these results and Pyrolysis -GC results (e.g., the absence of phenol in pyrolysates), the existence of C_{29}-steranes in the samples indicates a strong contribution to the proto-kerogen from green algae instead of the input of OM from terrestrial land plants (Moldowan et al. 1985). Additionally, extremely low sterane/hopane ratios (<0.19, Table 4b) imply the significant participation of bacteria during OM diagenesis, as well as biodegradation products (Peters et al. 2005).

Although further samples are accessible to a more thorough inquiry, in this research, no significant disparity was recorded between the obtained geochemical data concerning the source and environmental conditions. Consequently, it is presumed that the Sargelu oil shale in the Qalikuh area is comparable to the Garau oil shale. This is because they were both deposited in a marine depositional environment under continually distal marine circumstances with a rather constant source of OM.

Carbon isotope composition

For the Sargelu oil shale, the mean $\delta^{13}C$ values of saturated and aromatic HCs (Table 4a) were highly similar to those of the Garau oil shale, corresponding to the OM of the main marine origin since the difference between the fractions was less than 1.5-2‰ (cf. Sofer 1984). Furthermore, the $\delta^{13}C$ value of kerogen for the Sargelu samples was -27.67 and -28.24‰, reflecting a uniform origin. This statement is compatible with the extract results (i.e., the geochemistry data of the extracts).

As an accepted method, the isotope analysis of organic carbon can be applied to assess the origin and sedimentary environment of the sedimentary facies employing the $\delta^{13}C$ values of extract fractions (Collister and Wavrek 1996; Sofer 1984).

Thermal maturity of the oil shale

At the initial stages of catagenesis, the kerogen elemental ratios of the oil shale samples and maturity-related parameters from Rock-Eval data were used to delineate an early thermal maturity level (e.g., T_{max}, PI; Table 1). The biomarker ratios obtained (Table 4c) indicate that the Sargelu oil shale, like the Garau oil shale, was early mature and on the verge of entering the oil window (cf. Seifert and Moldowan 1980). For the Sargelu oil shale, the solid BRr (%) was employed as a petrographical maturation indicator because of the absence of vitrinite (Schoenherr et al. 2007). The early maturity level corresponding to the oil generation window was signified by the mean value of 0.43 BRr% offering an equivalent of 0.64 VRr% (Table 4b). Accordingly, an initial- to mid-level of maturation corresponds to the obtained MPI-1 value (0.68%) from the samples (Radke and Welte 1983). Moreover, the achieved 4-MDBT/1-MDBT ratios, which are just higher than 1.12 (Table 4c), reflect a maturity of 0.60% Rc (cf. Radke 1988). Regarding all employed approaches, the Sargelu oil shale has an early-to-moderate maturity level similar to the Garau oil shale.

Table 8. Comparison of the extracts composition, carbon isotope (δ^{13}), and molecular geochemistry results of the Sargelu and Garau oil shales in the Qalikuh area of the Zagros Mountains

Extracts composition, GC, and carbon isotope data	Sargelu oil shale (n=2)	Garau oil shale (n=3)	GC-MS Parameters	Sargelu oil shale (n=2)	Garau oil shale (n=3)
% Sat	7.29-10.13 (8.71)	7.07-9.48 (8.21)	DBT/phen	4.90-5.36 (5.13) ↑	2.95-4.25 (3.68) ↓
% Aro	38.08-43.20 (40.64) ↑	18.70-28.44 (23.21) ↓	$C_{31}R/C_{30}$ Hopane	0.41-0.45 (0.43)	0.41-0.42 (0.41)
% NSO	46.67-54.63 (50.65) ↓	62.08-73.20 (68.56) ↑	C_{29}/C_{30} Hopane	2.38-2.56 (2.47)	2.56-2.87 (2.71)
Pr/Ph	0.90-0.97 (0.93)	0.77-0.81 (0.78)	Gammacerane/ Hopane C_{30}	0.06-0.08 (0.07)	0.10-0.12 (0.11)
Pr/C_{17}	0.33-0.36 (0.34)	0.36-0.37 (0.37)	C_{27}/C_{29} Sterane	0.65-0.67 (0.66) ↓	0.98-1.09 (1.03) ↑
Ph/C_{18}	0.37-0.39 (0.38)	0.40-0.41 (0.40)	Sterane/ Hopane	0.14-0.19 (0.16)	0.15-0.18 (0.17)
CPI	0.48-0.48 (0.48)	0.23-0.48 (0.34)	22S/(22S+22R) C_{32} Hopane	0.57-0.59 (0.58)	0.58-0.59 (0.59)
δ^{13} C_{sat}	-27.37_-26.99 (-27.18)	-27.30_-26.94 (-27.07)	20S/(20S+20R) C_{29} Sterane	0.51-0.51 (0.51)	0.50-0.54 (0.52)
δ^{13} C_{aro}	-28.11_-27.91 (-28.01)	-27.83_-27.36 (-27.60)	MPI-1	0.68-0.68 (0.68)	0.50-0.58 (0.53)
δ^{13} kerogen	-28.24_-27.67 (-27.95)	-28.03_-27.64 (-28.09)	T_s/T_m	0.026-0.028 (0.027)	0.014-0.015 (0.014)
	This study	Shekarifard et al. 2019		This study	Shekarifard et al. 2019

n: number of investigated samples; range (mean); for abbreviation refer to Table 4.

Conclusions

The Qalikuh oil shales (i.e., the Sargelu and Garau oil shales) are highly similar in terms of geochemistry, mineralogy, and pyrolysate products despite their different stratigraphy and age. This suggests profound time-transgressive paleo-depositional stability.

The Sargelu oil shale is early mature organic-rich facies (mean TOC: 15.47 wt%) with high quality (mean S_2: 84 mg HC/g rock; mean HI: 548 mg HC/g TOC). The kerogen of the Sargelu oil shale primarily consists of amorphous OM (AOM), which is deposited under an anoxic marine condition in a carbonate environment. Type II-S kerogen is documented for the Sargelu oil shale as well.

The Qalikuh oil shales are, in fact, bitumen-rich carbonate rocks and display no typical physical properties of ideal shale stones. Compared to the Garau oil shale, the Sargelu oil shale has only a slightly higher content of argillaceous minerals and pyrite framboids.

The Qalikuh oil shale is capable of producing and expelling light oil for the Jurassic-Cretaceous petroleum systems in the Zagros Basin, in addition to acting as shale gas reservoirs where they are deeply buried and highly matured. the separation of the Sargelu-derived oil from the Garau-derived oil is a major challenge in the conventional petroleum systems of Iran, where Sargelu and Garau formations act as effective SRs.

Despite a great similarity between these organic facies, the results of this study show that the ratios of DBP/Phen and C_{27}/C_{29} sterane can be used to recognize the Sargelu-derived oils from the Garau-derived oils. The Sargelu-derived oils show a higher ratio of DBP/Phen and a lower ratio of C_{27}/C_{29} sterane in comparison with the Garau-derived oils. Finally, these critical geochemical parameters can be applied for a better understanding of the Jurassic-Cretaceous petroleum systems in the Zagros Basin.

Acknowledgements

We would like to highly express our gratitude to the National Iranian Oil Company (Exploration Directorate) for their support, motivations during the research, and the permission for data publication. The KEPS company is acknowledged for their logistic supports during fieldtrips.

Conflict of Interests: The authors declare no conflict of interest.

References

Abdula R.A. 2015. Hydrocarbon potential of Sargelu Formation and oil source correlation, Iraqi Kurdistan. Arabian Journal of Geosciences 8: 5845-5868.

Ala MA, Kinghorn RRF, Rahman M (1980) Organic geochemistry and source rock characteristics of the Zagros Petroluem Province, southwest Iran. Journal of Petrolum Geology 3: 61-89.

Alan W., 1969 The crush zone of the Iranian Zagros Mountain Range, and its implications. Geological Magazine 106: 385-394.

Agard P., Omrani J., Jolivet L., Mouthereau F,. 2005. Convergence history across Zagros, Iran; constraints from collisional and earlier deformation. International Journal of Earth Sciences 94: 401-419.

Ayres M.G., Bilal M., Jones R.W., Slentz L.W. et al 1982. Hydrocarbon habitat in main producing areas, Saudi Arabia. AAPG Bull., 66: 1-9.

Behar F., Beaumont V., Penteado H.D.B., 2001. Rock-Eval 6 technology: performances and developments. Oil and Gas Science and Technology, 56: 111-134.

Berberian M., 1995. Master "blind" thrust faults hidden under the Zagros folds: active basement tectonics and surface morphotectonics. Tectonophysics, 241: 193-224.

Berberian M, King G., 1981. Towards a paleogeography and tectonic evolution of Iran. Canadian journal of earth sciences, 18: 210-265.

Bordenave M., Burwood R., 1990. Source rock distribution and maturation in the Zagros orogenic belt:

provenance of the Asmari and Bangestan reservoir oil accumulations. Organic Geochemistry, 16: 369-387.
Bordenave M, Hegre J.A. 2005. The influence of tectonics on the entrapment of oil in the Dezful Embayment, Zagros Fold belt, Iran. Journal of Petroleum Geology, 28: 339-368.
Bordenave M.L., Hegre J.A. 2010. Current distribution of oil and gas fields in the Zagros Fold Belt of Iran and contiguous offshore as the result of the petroleum systems. Geological Society, London, Special Publications, 330 (1): 291-353.
Bordenave M.L., Huc A.Y. 1995 The cretaceous SRs in the Zagros foothills of Iran. Oil & Gas Science and Technology 50(6): 727-752.
Collister J, Wavrek D., 1996. $\delta^{13}C$ compositions of saturate and aromatic fractions of lacustrine oils and bitumens: evidence for water column stratification. Organic Geochemistry 24, 913-920.
Didyk B, Simoneit B., 1978 Organic geochemical indicators of palaeoenvnonmental conditions of sedimentation. Nature 272: 216-222.
Eglinton TI, Sinninghe DJS et al (1990) Rapid estimation of the organic sulphur content of kerogens, coals and asphaltenes by pyrolysis-gas chromatography. Fuel 69, 1394-1404.
England WA, Mackenzie AS (1989) Some aspects of the organic geochemistry of petroleum fluids: Geologische Rundschau 78 (1): 291–303.
England WA, Mackenzie AS., 1987. The movement and entrapment of petroulem fluids in the subsurface. Journal of Geological Society 144, 327-347.
Erbacher J, Thurow J, Littke R 1996. Evolution patterns of radiolaria and organic matter variations: a new approach to identify sea-level changes in mid-Cretaceous pelagic environments. Geology, 24(6): 499-502.
Fatah SS, Mohialdeen I.M., 2016. Hydrocarbon generation potential and thermal maturity of Middle Jurassic Sargelu Formation in Miran Field, Sulaimani Area, Kurdistan Region, NE Iraq. Journal of Zankoy Sulaimani, Special Issue, GeoKurdistan II, 213-228.
Hesselbo S.P., Grocke D.R., 2000. Massive dissociation of gas hydrate during a Jurassic oceanic anoxic event. Nature, 406 (6794): 392-395.
Horsfield B (1989) Practical criteria for classifying kerogens: some observations from pyrolysis-gas chromatography. Geochimica et Cosmochimica Acta 53: 891-901.
Huang WY, Meinschein W (1979) Sterols as ecological indicators. Geochimica et Cosmochimica Acta 43: 739-745.
Hunt J.M., 1996. Petroleum geochemistry and geology. 2nd ed., W. H. Freeman and Company, 743 pp.
Jenkyns HC., 1980. Cretaceous anoxic events: from continents to oceans. Journal of the Geological Society, 137(2):171-188.
Kamali MR, Rezaee M.R., 2003. Burial history reconstruction and thermal modeling at Kuh-Mond, SW Iran. Journal of Petroleum Geology 26: 415–464.
Karlsen DA, Skeie JE. 2006. Petroleum Migration, Faults and Overpressure, Part I: Calibrating Basin Modelling using Petroleum in Traps - a Review, Journal of Petroleum Geology 29 (3): 227–256.
Killops VJ, Killops SD. 2013. Introduction to organic geochemistry. John Wiley & Sons.
Klemme, H.D., 1994. Petroleum systems of the world involving Upper Jurassic SRs. In: Magoon LB, Dow WG (eds) The petroleum system—from source to trap, AAPG Memoir 60, Tulsa, 51–72.
Kondner RB, Pearson A et al 2008. Sterols and interpreting Paleozoic steranes Sterols in red and green algae: quantification, phylogeny, and relevance for the interpretation of geologic steranes. Geobiology 6: 411-420.
Larter SR (1984) Application of analytical pyrolysis techniques to kerogen characterisation and fossil fuel exploration/exploitation. In: Voorhees, K. (Ed.), Analytical pyrolysis, methods and applications. Butterworth, London, 212-275.
Leckie RM, Bralower TJ, Cashman R (2002) Oceanic anoxic events and plankton evolution: Biotic response to tectonic forcing during the mid-Cretaceous. Paleoceanography, 17(3): 13-1.
Mahbobipour H, Kamali MR, Solgi A (2016) Organic geochemistry and petroleum potential of Early Cretaceous Garau Formation in central part of Lorestan zone, northwest of Zagros, Iran. Marine and Petroleum Geology 77, 991-1009.
Moldowan JM, Fago FJ (1986) Structure and significance of a novel rearranged monoaromatic steroid hydrocarbon in petroleum. Geochimica et Cosmochimica Acta 50: 343-351.
Moldowan JM, Seifert WK, Gallegos EJ (1985) Relationship between petroleum composition and

depositional environment of petroleum SRs. AAPG bull., 69, 1255-1268.
Montero-Serrano JC, Bout-Roumazeilles V et al (2010) Changes in precipitation regimes over North America during the Holocene as recorded by mineralogy and geochemistry of Gulf of Mexico sediments. Global and Planetary Change 74, 132-143.
Motiei H (1993) Treatise on the geology of Iran: Stratigraphy of Zagros. Geological Survey of Iran, Tehran.
Murris RJ (1980) Middle East: stratigraphy and oil habitat. AAPG Bull., 64, 597-618.
Omar N, McCann T et al (2021) Solid bitumen in shales from the Middle to Upper Jurassic Sargelu and Naokelekan Formations of northernmost Iraq: implication for reservoir characterization. Arabian Journal of Geosciences, 14(9), 1-20.
Peters KE, Cassa MR (1994) Applied source rock geochemistry. In: Magoon LB, Dow WG (eds) The petroleum system—from source to trap, vol 60. AAPG Memoir, Tulsa, 93–120
Peters KE, Clifford C, Moldowan JM (2005) The Biomarker Guide, 2nd ed. Prentice Hall, New Jeresy.
Peters KE, Moldowan JM (1993) The biomarker guide: interpreting molecular fossils in petroleum and ancient sediments. Prentice-Hall, Englewood Cliffs, NJ.
Peters KE, Hostettler FD et al (2008) Families of Miocene Monterey crude oil, seep, and tarball samples, coastal California: AAPG Bull., 92(9), 1131- 1152.
Radke M, Welte D (1983) The Methylphenanthrene Index (MPI): A Maturity Parameter Based on Aromatic Hydrocarbons. Advances in Organic Geochemistry, 1983, 1981, 504-512.
Radke M (1988) Application of Aromatic Compounds as Maturity Indicators InSRs and Crude Oils. Marine and Petroleum Geology. 5, 224-236
Rasouli A, Shekarifard A et al (2015) Occurrence of organic-rich deposits (Middle Jurassic to Eraly Cretaceous) from Qalikuh locality, Zagros Basin, South-West of Iran: A possible oil shale resource. International Journal of Coal Geology 143, 34-42.
Riboulleau A, Schnyder J et al (2007) Environmental change during the Early Cretaceous in the Purbeck-type Durlston Bay section (Dorset, Southern England): a biomarker approach. Organic Geochemistry 38, 1804-1823.
Sales JK (1997) Seal Strength vs. Trap Closure - A Fundamental Control on the Distribution of Oil and Gas, in R.C. Surdam, ed., AAPG Memoir, 67, 57–83.
Schoenherr J, Littke R et al (2007) Polyphase thermal evolution in the Infra-Cambrian Ara Group (South Oman Salt Basin) as deduced by maturity of solid reservoir bitumen. Organic Geochemistry 38, 1293-1318.
Seifert WK, Moldowan JM (1978) Applications of steranes, terpanes and monoaromatics to the maturation, migration and source of crude oils. Geochimica et Cosmochimica Acta 42: 77-95.
Seifert W.K., Moldowan JM (1980) The effect of thermal stress on source-rock quality as measured by hopane stereochemistry. Physics and Chemistry of the Earth 12, 229-237.
Shekarifard A., Daryabandeh M. et al, 2019.Petroleum geochemical properties of the oil shale from the Eraly Cretaceous Garau Formation, Qalikuh locality, Zagros Mountain Range, Iran. International Journal of Coal Geology, 206: 1-18.
Sofer Z., 1984. Stable carbon isotope compositions of crude oils: application to source depositional environments and petroleum alteration. AAPG Bull., 68: 31-49.
Stasiuk L., Goodarzi F., Bagheri-Sadeghi H., 2006. Petrology, rank and evidence for petroleum generation, upper Triassic to Middle Jurassic coals, central Alborz Region, Northern Iran. InternationalJournal of Coal Geology, 67: 249-258.
Stoneley R. 1987. A review of petroleum SRs in parts of the Middle East. Geological Society, London, Special Publications, 26: 263-269.
Taylor G, Teichmuller M, Davis A et al 1998. Organic Petrology. Gebrüder Borntraeger, Berlin, Stuttgart.
Tissot B.P., Pelet R, Ungerer Ph. 1987 Thermal history of sedimentary basin, maturation indices, and kinetics of oil and gas generation, AAPG Bull., 71 (12): 1455-1466.
Tissot BP, Welte DH (1984) Petroleum Formationand Occurrence. 2nd ed., Springer Verlag, Berlin.
Van Buchem F., Baghbani D. et al 2010. Barremian-Lower Albian sequence-stratigraphy of southwest Iran (Gadvan, Dariyan and Kazhdumi formations) and its comparison with Oman, Qatar and the United Arab Emirates. GeoArabia Special Publication, 4 (2): 503-548.
Volkman J.K., Alexander R. et al 1983, Demethylated hopanes in crude oils and their applications in

petroleum geochemistry. Geochimica et Cosmochimica Acta, 47: 785-794.
Ziegler M.A., 2001, Late Permian to Holocene paleofacies evolution of the Arabian plate and its hydrocarbon occurrences. GeoArabia, 6: 445-503.